Kinetic modelling of runaways in fusion plasmas

T. Fülöp,[1], O. Embréus[1], A. Stahl[1], S. Newton[1,2], I. Pusztai[1] and G. Wilkie[1]

[1]Department of Physics, Chalmers University of Technology, Göteborg, Sweden
[2]CCFE, Culham Science Centre, Abingdon, Oxon, OX14 3DB, UK

Corresponding Author: tunde@chalmers.se

Abstract:
Mitigation of runaway electrons is one of the outstanding issues for a reliable operation of ITER and other large tokamaks. To achieve this, quantitatively accurate estimates for the expected runaway electron energies and current are needed. In this work we describe an accurate theoretical framework for studying the effects of collisional nonlinearities, bremsstrahlung and synchrotron radiation emission, and knock-on collisions on the runaway electron distribution. We outline the identification of significant features of runaway electron behaviour enabled by this framework and their potential to affect the growth of a runaway population.

1 Introduction

ITER requires an effective control system for runaway electrons (REs) [1, 2], which form when a strong electric field allows the high velocity region of the electron population to detach from the thermal bulk, due to the velocity dependence of the collisional friction experienced by plasma particles. A primary, or seed, population of fast electrons grows exponentially by the avalanche mechanism, resulting from close collisions between fast and thermal electrons. The necessary electric field can arise during disruptions [3], as the plasma temperature drops from the typical operating regime of around several keV to 10 eV or less in a few milliseconds. A large electric field is initially induced parallel to the magnetic field to maintain the megaamperes of confining current at the pre-disruption level. This field can decay rapidly in response to the formation of a narrow runaway electron beam with particle energies up to tens of MeV, which carries a significant fraction of the current. The potential for damage by such a localised, high energy beam on contact with the vessel wall is large, and must be reduced using mitigation techniques.

In this work we describe an accurate theoretical framework for studying the effects of collisional nonlinearities, bremsstrahlung and synchrotron radiation emission, and knock-on collisions on the RE distribution. Kinetic simulation is the most accurate and useful method for investigating RE dynamics and we use the continuum tool CODE (COllisional Distribution of Electrons) [4, 5] to solve the spatially homogeneous kinetic equation for

electrons in 2D momentum space. CODE is well-suited for fast and detailed study of the above mentioned processes. It is able to accurately model sub-Dreicer electric-field acceleration, collisions, avalanche RE generation, and synchrotron and bremsstrahlung radiation losses for electrons with arbitrary energies. CODE has been used to study hot-tail generation of runaways [5], the spectrum of the synchrotron and bremsstrahlung radiation emitted by runaways, the corresponding influence of the emission on the distribution function [6–8], and the factors influencing the critical electric field for RE generation [9].

In addition, we recently developed a fully nonlinear relativistic tool, that can be used even when the runaway population becomes comparable to the thermal population or when the electric field is of the order of the Dreicer field E_{D}. The new finite-difference code NORSE (NOn-linear Relativistic Solver for Electrons) [10], solves the kinetic equation in 2D momentum space (as CODE), including electric-field acceleration and synchrotron radiation reaction, but uses a fully relativistic non-linear Fokker-Planck operator [11]. The operator in NORSE is valid for collisions between electrons of arbitrary energy. Therefore, it relaxes limitations such as that the bulk population should be non-relativistic; in fact, no arbitrary distinction between bulk and runaway populations is necessary. A 2D non-uniform finite-difference grid is used to represent momentum space, however when evaluating the five relativistic potentials (analogous to the two Rosenbluth potentials in the non-relativistic case), a mixed finite-difference–Legendre-mode representation is used as the potentials are given by simple 1D integrals in a Legendre-mode decomposition. The ability to handle time-dependent plasma parameters makes the investigation of dynamic scenarios possible in both CODE and NORSE. In the following sections we outline recent achievements in runaway electron modelling with this code set.

2 Radiative processes

The emission of electromagnetic radiation by a charged particle in accelerated motion is associated with a reduction in its energy, accounted for by the inclusion of a radiation reaction force in the kinetic equation. For REs in plasmas, the dominant radiative processes are the emission of bremsstrahlung and synchrotron radiation.

Synchrotron radiation Recent work using the kinetic equation solvers CODE and LUKE showed that the synchrotron radiation reaction can lead to bump-on-tail formation, where relativistic electrons accumulate at a certain energy [6, 7]. The dynamics is set by the interplay of the pitch-angle scattering of the accelerated population to higher perpendicular momenta with the synchrotron radiation back-reaction, which becomes more effective in slowing down the electrons as the pitch of the particle increases. The pitch-angle scattering will lead to an exponential decay of the electron distribution function in the far tail. The accelerated electrons will return to the "runaway region" (defined as the region where the convective momentum balance is positive, i.e. where the particles are gaining momentum) due to collisional friction and radiation reaction and they create a bump in the distribution function. This bump feature leads to stronger gradients in the perpendicular direction and presents a potential source for kinetic instabilities, which can play a role in limiting the formation of large runaway beams [12–15]. The location of the synchrotron

bump in momentum space can be estimated from the following formula [7, 17]

$$p_{\mathrm{B}} \approx 320 \frac{n_{20}}{B^2} \frac{E/E_{\mathrm{c}}(E/E_{\mathrm{c}}-1)}{Z_{\mathrm{eff}}+1}, \tag{1}$$

where $p = \gamma v/c$ is a normalized momentum, n_{20} is the electron density in units of 10^{20} m^{-3}, B is the magnetic field in T, and E_{c} is the critical electric field for runaway generation [18]. The bump location in units of MeV is almost exactly $p_{\mathrm{B}}/2$. From earlier test-particle studies, the pre-factor was estimated at 230 [17], but from an extensive numerical parameter scan using CODE, we find the value 320 for the location of the maximum of the bump in f. p_B might not necessarily agree exactly with the average energy of the bump electrons, but gives the right order of magnitude. For the parameters of current experiments (e.g. DIII-D), p_B is expected to be above 100 MeV. Since REs with such high energies do not appear to be present in current experiments (as they are likely to be lost before they are accelerated to these energies), the synchrotron bump is probably difficult to observe experimentally.

Bremsstrahlung radiation Starting from the Boltzmann transport equation, we recently derived a collision operator which describes the bremsstrahlung radiation reaction, fully accounting for the finite energy and emission angle of the emitted photons [8]. We have implemented the operator in CODE, and used it to study the effect of bremsstrahlung on the distribution of electrons in 2D momentum-space. As a consequence of the complicated momentum-space dynamics in the presence of radiation reaction, non-monotonic features in the RE tail can be observed. We found significant differences in the distribution function when bremsstrahlung losses were modelled with a Boltzmann equation (the "Boltzmann" model) compared to the model typically used, where only the average bremsstrahlung friction force is accounted for (the "mean-force" model).

Figure 1 shows the steady-state electron distribution function in momentum space, with full Boltzmann bremsstrahlung radiation reaction effects (black, solid), compared to that from the mean-force model used in previous work [17, 20] (red, solid). The Boltzmann bremsstrahlung operator allows the REs to reach much higher energies than the previously used mean-force model, although the average runaway-electron energy is almost the same in the Boltzmann and mean-force cases. The difference is due to the fact that in the Boltzmann model, the emission is treated as discrete events where some electrons suddenly lose a large part of their total energy, while some are accelerated for a long time without any losses. This creates the large spread in energy. In the mean-force model, each electron experiences the average energy loss continuously, giving rise to a sharp feature, located where the energy gain due to the electric-field acceleration balances friction and bremsstrahlung losses.

Another difference between the Boltzmann and mean-force models is the emergence of a population of fast electrons with significant perpendicular momentum but at lower parallel momenta. This is due to emission of low energy photons in interactions with ions. The blue dashed lines in Figure 1 demonstrates this by showing the distribution resulting from an approximate model based on the Boltzmann operator, but neglecting the deflection of the electrons in the bremsstrahlung reactions due to the emission of soft

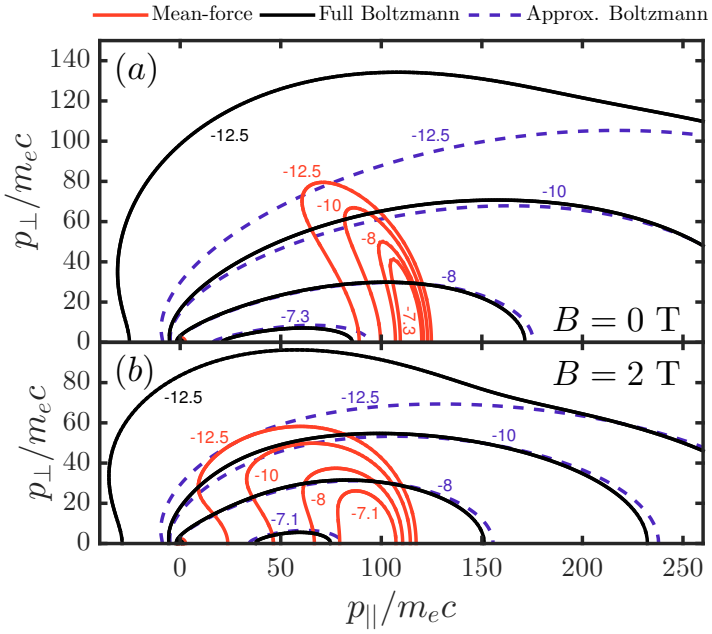

FIG. 1: Steady-state electron 2D distribution functions with (a) no magnetic field and (b) $B = 2$ T. The other parameters are electric field $E = 2E_c$, effective charge $Z_{\text{eff}} = 10$, electron density $n_e = 3 \cdot 10^{21}\, m^{-3}$ and temperature $T_e = 10\, keV$. Contours of $\log_{10} F$ are shown, where $F = (2\pi m_e T_e)^{3/2} f_e / n_e$.

photons. These bremsstrahlung interactions carry very little energy but they contribute to angular deflection. It may seem counter-intuitive that low energy photon emissions contribute to large angle collisions but since there is a large mass difference between the electron and ion, large momentum transfers are allowed even without energy transfer.

When synchrotron radiation losses are included (Fig. 1b), the qualitative features remain the same. The momentum-space distribution is shifted towards lower energies, as expected. The difference between the Boltzmann and mean force models is reduced but it is still substantial. Note that the impact of bremsstrahlung becomes important compared to synchrotron effects when $n_{20}(E/E_c)/B^2 > 1$, and a synchrotron bump is much more likely to form in fusion relevant plasmas. A "dynamic bump", caused by changing plasma parameters could also potentially form and "travel" towards higher energies as a coherent feature in the distribution.

3 Effect of nonlinear collision operator

The electric field is expected to reach values as high as 80-100 V/m during the current quench in ITER [19], and runaway generation may be strong enough for a substantial fraction of the plasma current to be converted to runaway current. Under these circumstances, the distribution function may not be close to a Maxwellian, in which case the

linearization of the collision operator breaks down. If the electric field is strong enough, the net force parallel to the magnetic field experienced by electrons due to the electric field and collisions becomes positive in the entire momentum space, which leads to a phenomenon known as electron "slide-away". The slide-away process cannot be modelled using linear tools (such as CODE or LUKE), since they assume a Maxwellian background plasma.

A strong electric field represents a source of energy that quickly heats up the electron distribution, thereby making a bigger population prone to be accelerated. In practice, this heating is balanced by many processes which act to remove heat from the plasma. There is a wealth of experimental evidence for the differences in the radiated energy to affect the energy spectrum of the runaways, see e.g. [2, 21]. In a cold post-disruption plasma, line radiation and bremsstrahlung from interaction with partially ionized impurities are important loss channels, as is radial heat transport. Including a heat sink in numerical simulation of such scenarios is therefore desirable. Figure 2 highlights the importance of the heat sink by comparing the electron distribution obtained with and without a heat sink applied, at two different times. Clearly, in the case without a heat sink, the bulk heating leads to a strong departure from the Maxwellian, despite the fact that the electric field is much less than the Dreicer field.

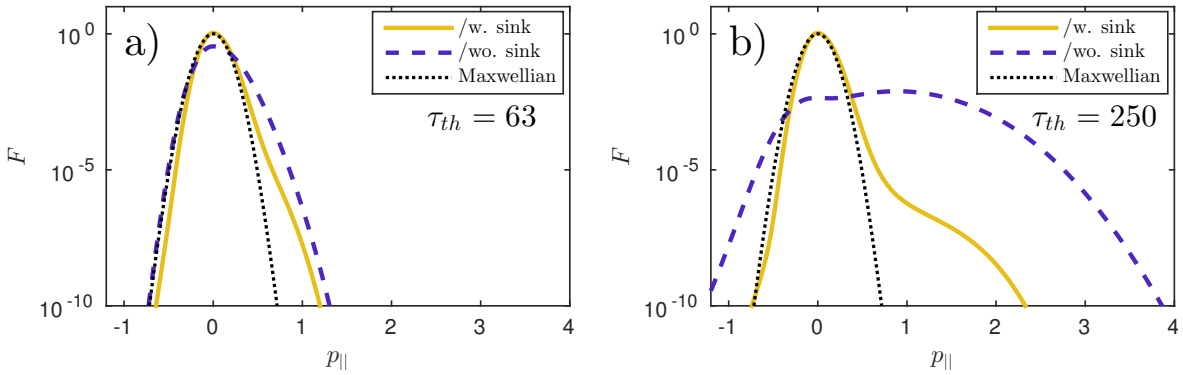

FIG. 2: Cut along the parallel axis of the distribution function after a) 63 and b) 250 thermal collision times in a NORSE *run with a constant electric field of* $E = 0.15$ V/m. $n_e = 5 \cdot 10^{19}$ m^{-3}, $Z_{eff} = 1$ *and* $B = 0$ T *were used, and with the initial temperature* $T_e = 5.11$ keV, *the electric field corresponds to* $E/E_D = 0.035$ *and* $E/E_c = 3.5$. *The distributions are normalized to their initial maximum value.*

More generally, our results show that the evolution of the runaway electron population is sensitive to the properties of the heat sink. If the heat sink is able to successfully maintain the bulk plasma temperature, the runaway population grows steadily by means of the Drecier mechanism, slowly depleting the thermal population until eventually all particles are runaways (provided that the electric field is maintained). If the heat sink has a limited energy removal rate (or is otherwise less than ideal), the resulting heating of the bulk leads to an increase in the effective normalized electric field. Eventually, a positive feedback mechanism sets in by means of which the bulk is quickly depleted, reducing the friction on the thermal population until the point where the slide-away is reached. This

process can be initiated at significantly weaker fields than expected from linear theory. The sensitivity to the details of the heat sink makes a more detailed investigation of various energy loss channels an area of interest for future work.

The importance of the details of the heat-loss channels has far-reaching consequences for the understanding of runaway-electron dynamics. The absence of a heat-sink might lead to a transition to the slide-away regime, which in turn will impact the subsequent electric-field evolution, leading to a reduction in field strength and duration. Therefore, it is difficult to determine the magnitude of the effect of collisional nonlinearities on the RE current evolution without a self-consistent calculation of the heat-losses, the electron distribution and the electric field.

4 Runaway avalanches

Avalanche runaway generation is the phenomenon whereby REs are generated due to large-angle collisions of already existing REs with thermal electrons, leading to an exponential growth of the runaway current. As the secondary runaway generation is proportional to the density of existing runaways, the dynamics can be non-linear, and small variations in the balance between runaway generation and losses can lead to large differences in the resulting runaway fraction and determine whether a significant runaway beam is formed or not [22].

The large-angle collisions are not described by the Fokker-Planck collision operator commonly employed, and are instead accounted for by the addition of a particle source term in the kinetic equation [23, 24]. The most commonly used operator, derived in Ref. [23], assumes that the momentum of the incoming particle is infinite and its pitch-angle is vanishing ($p_\perp = 0$). This implies that the incoming particle is unaffected by the interaction, and that all runaways contribute equally strongly to the avalanche process. This has the non-physical consequence that particles can be created at energies higher than that of any of the existing runaways. The operator derived in Ref. [24] relaxes some

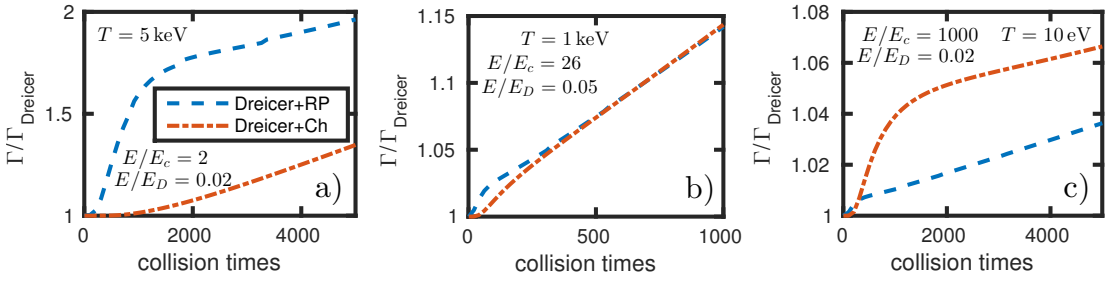

FIG. 3: Runaway growth rates normalized to the Dreicer growth rate for three different scenarios. Blue dashed and red dash-dotted are for the avalanche source terms in Ref. [24] and Ref. [23], respectively. Substantial changes between the two operators can be expected either when the temperature is high and the electric field is low (Ref. [23] over-predicts) or when the temperature is low and the electric field is large (Ref. [23] under-predicts).

of these assumptions. It still assumes that all incoming particles have zero pitch-angle but takes their energy distribution into account. The momenta of the outgoing particles are restricted through momentum conservation. Both of these operators are implemented in CODE [5] and by studying the runaway generation process we find that the more accurate operator (Chiu-Harvey [24]) produces more runaways when the temperature is low and E/E_c large (see Fig. 3). This means that a typical ITER disruption would lead to higher avalanche growth rates than the simpler operator (Rosenbluth-Putvinski [23]) predicts.

A physically more accurate large-angle collision operator can be derived in the high-energy limit of the linearized relativistic Boltzmann collision integral. This operator generalizes previous models of large-angle collisions to model the slowing-down of the incident primary electrons, and accounts for the full momentum dependence of the primary distribution, and also conserves particle nun

Figure 4 compares the RE growth rate given by the fully conservative Boltzmann operator with that of the Chiu-Harvey model. Using plasma parameters $T = 100\,\mathrm{eV}$, $n = 1 \cdot 10^{20}\,\mathrm{m}^{-3}$ and $Z = 3$, the distribution function is evolved in time until the growth rate approaches a steady-state value, which occurs after approximately 200 ms.

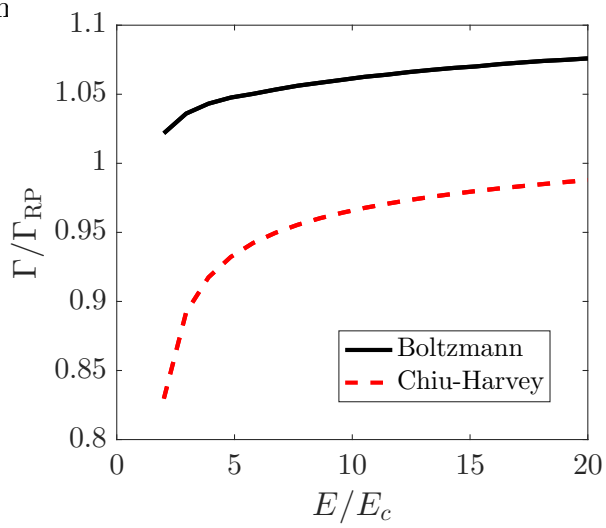

FIG. 4: Avalanche growth rate as function of electric field using different models for the avalanche source rate, normalized to values obtained in the Rosenbluth-Putvinski model.

The growth rate obtained with the Boltzmann model differs from the Chiu-Harvey model because of three effects: a decrease caused by the additional slowing-down provided by accounting for the energy loss of the primary electron in the knock-on collision; a slight decrease due to accounting for the full pitch-angle dependence of the primary distribution; and an increase by reducing the Coulomb logarithm in the Fokker-Planck operator in order to avoid double counting collisions. The net result is a growth rate increased by up to 20% compared to the Chiu-Harvey model.

5 Conclusions

Runaway electrons (REs) are a pressing issue for ITER due to their significant potential to cause damage. Improved knowledge of RE formation mechanisms, their dynamics and characteristics, as well as transport or loss processes that may contribute to RE suppression and control, will benefit the fusion community and contribute to a safe and reliable operation of reactor-scale tokamaks.

We report on recent developments of the continuum kinetic tools used to model REs, CODE and NORSE, outlining the identification of important features of RE be-

haviour which these developments enable. Radiation back reaction due to synchrotron and bremsstrahlung, which limit the highest runaway energies, can lead to the development of non-monotonic electron distributions. The form of the RE distribution is found to be sensitive to the applied bremsstrahlung model. Using the most sophisticated implementation based on a Boltzmann collision model demonstrates the importance of accounting for the discrete nature of the bremsstrahlung events, and for the electron scattering due to the emission of soft photons. The nonlinear fully relativistic Fokker-Planck collision operator of NORSE is employed to study full distribution slide-away situations accelerated by the heating of the bulk distribution. Furthermore, a systematic comparison of various secondary generation models points to the importance of taking kinematic constraints of large angle scattering events into account, for the accurate evaluation of the avalanche growth rate.

Acknowledgment The authors are grateful to G. Papp and M. Landreman for fruitful discussions. This work was supported by the Swedish Research Council (Dnr. 2014-5510), and the European Research Council (ERC-2014-CoG grant 647121).

References

[1] M. Lehnen, A. Alonso, G. Arnoux *et al*, Nucl. Fusion **51** 123010 (2011).
[2] E. M. Hollmann, P. Aleynikov, T. Fülöp *et al*, Phys. Plasmas **22** 021802 (2015).
[3] E. M. Hollmann, M. E. Austin, J. A. Boedo *et al*, Nucl. Fusion **53** 083004 (2013).
[4] M. Landreman, A. Stahl and T. Fülöp, Comp. Phys. Comm. **185** 847 (2014).
[5] A. Stahl, O. Embréus, G. Papp *et al*, Nucl. Fusion **56** 112009 (2016).
[6] E. Hirvijoki, I. Pusztai, J. Decker *et al*, J. Plasma Phys. **81** 475810504 (2015).
[7] J. Decker, E. Hirvijoki *et al*, Plasma Phys. Control. Fusion **58** 025016 (2016).
[8] O. Embréus, A. Stahl and T. Fülöp, New Journal of Physics **18** 093023 (2016).
[9] A. Stahl, E. Hirvijoki, J. Decker *et al*, Phys. Rev. Lett. **114** 115002 (2015).
[10] A. Stahl, O. Embréus *et al*, Submitted to Comp. Phys. Comm. (2016). http://arxiv.org/abs/1608.02742
[11] B. J. Braams, C. F. F. Karney, Phys. Fluids B: Plasma Phys. **59** 1355 (1989).
[12] T. Fülöp, G. Pokol, P. Helander *et al*, Phys. Plasmas **13** 062506 (2006).
[13] G. Pokol, T. Fülöp and M. Lisak, Plasma Phys. Control. Fusion **50** 045003 (2008).
[14] A. Kómár, G. Pokol and T. Fülöp, Phys. Plasmas **20** 012117 (2013).
[15] T. Fülöp and S. Newton, Phys. Plasmas **21** 080702 (2014).
[16] P. Aleynikov and B. Breizman, Nucl. Fusion **55** 043014 (2015).
[17] I. Fernández-Gómez *et al*, Phys. Plasmas **14** 072503 (2007).
[18] J.W. Connor and R.J. Hastie, Nucl. Fusion **15** 415 (1975).
[19] H. Smith, P. Helander, L.-G. Eriksson *et al*, Phys. Plasmas **13** 102502 (2006).
[20] M. Bakhtiari *et al*, Phys. Rev. Lett. **94** 215003 (2005).
[21] G. Papp, T. Fülöp, T. Fehér *et al*, Nucl. Fusion **53** 123017 (2013).
[22] T. Fülöp, H. M. Smith and G. I. Pokol, Phys. Plasmas **16** 022502 (2009).
[23] M. N. Rosenbluth and S. Putvinski, Nucl. Fusion **37** 1355 (1997).
[24] S. C. Chiu, M. N. Rosenbluth, R. W. Harvey *et al*, Nucl. Fusion **38** 1711 (1998).